

# A Novel Single Switch High Step Up DC-DC Converter for PV Based Application

T. Arunkumari\*, V.Indragandhi\*\*‡

\*School of Electrical Engineering, Research Scholar, VIT University, Vellore.

\*\* School of Electrical Engineering, Associate Professor, VIT University, Vellore.

(aak.thi90@gmail.com, arunindra08@gmail.com)

‡ V.Indragandhi; VIT University , Tel: 9750603539

Arunindra08@gmail.com

*Received: 21.08.2017 Accepted:24.12.2017*

**Abstract** - A new converter of single switch mode with high step up ratio is proposed in this manuscript. The proposed converter design is a combination of Voltage Tripler (VT) and sepic boost converter. This design uses MOSFET switch with reduced switching and conduction loss. Converter achieves high step up voltage gain with appropriate duty cycle and less voltage strain on the switch. The energy stored in the inductor can be recycled towards the output capacitor. The working condition of the converter under Continuous Conduction Mode (CCM) is given in detail. The input of 30V of PV source is boosted to 400V by this proposed converter. The main advantage of the proposed converter is single switch, reduced component stress and size, the ripple current and voltage is less. The efficiency attained is 93%. The simulation of this converter is done using MATLAB Simulink.

**Keywords:** Boost converter, CCM, high voltage gain, Single switch, voltage Tripler.

## 1. Introduction

Renewable energy is increasing rapidly and plays a very important role in production and distribution system. This energy system gives an option for the consumer to choose whether they want to utilize the utility power or micro-source power. Even they can act as the main producer of the renewable power at the location they need with the help of micro-grid technology [1]. This technology normally comprises several micro-sources such as PV, Wind, bio fuel etc. and heaps, which works as an autonomous and manageable scheme when they are connected in either grid-connected mode or islanded mode [2].

The PV power sources are generated for both stand alone and grid connected applications below the distributed mode [3]. The circulating currents are produced while generating the power from renewable sources and these currents are suppressed by autonomous control. In [4] the author has proposed multilayer control on microgrid providing a balanced power with reduction in peak consumption value of the grid. Proposal of the power

architecture is given in [5] which is utilized for the application of electric vehicle and also details about the integration to grid with the help of electric vehicle. In [6] synchronization with smooth effect of grid and microgrid is proposed which is utilized for both stand alone and grid connected states.

In nature, the PV sources are capable of producing low dc voltage hence it is not suitable for direct connection to microgrid. To improve the voltage level, PV modules are connected in series. Hence it results in the large area and increased number of PV devices. To demolish this drawback the usage of DC-DC converter is required. The DC-DC converters are not only overcomes the draw-back; it is also very helpful in stepping up the low voltage level to high voltage range with good efficiency. It's helpful in utilizing renewable energy resources in a better way [7]. The major requirements of the converter are low cost, less weight, less voltage strain in switch, high density power. The block diagram of the scheme is represented in fig. 1

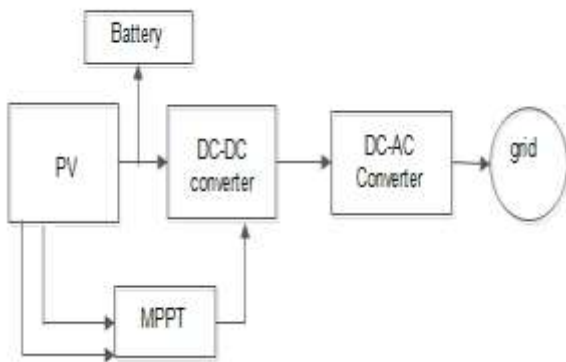


**Fig. 1** Block diagram of PV system

The major classification of the DC-DC converter is isolated and non-isolated converts depending on high voltage conversion ratio. Isolated converter type has a transformer model in it. The high voltage gain is attained by changing the turns of the transformer. The isolated converters are many and some of them are, fly-back, push-pull, fly-forward converter [8, 9]. The isolated converters have a common drawback of high voltage stress due to the inductive leakage in the transformer which affects the efficiency of the converter directly [10]. Under the classification of non-isolated converters conventional boost converter delivers high voltage gain ratio with by utilizing large duty cycle resulting in high switching voltage stress which in turn reducing the efficiency of the system [11].

So in order to increase the efficiency of the non-isolated converters, many designs are proposed. First couple inductor method has been in existence to improve the efficiency [12, 13]. It is attained by tuning the turns of the turns ratio of the inductive coupler as same as converter with the transformer. But due to leakage in inductance switch is affected due to voltage stress and strain. As a next step to overcome this problem active and passive clamping methods was in use. This technique is used along with coupled inductive method [14]. But the cost and size is increased. To improve the overall system, switched capacitor technique is implemented [15-16]. Switched capacitor is aligned at the switching condition of the DC converter to attain high voltage ratio with required duty cycle. But one major drawback of this technique is, a pulsating input current is produced which leads to poor line and load problems. The circuit becomes complex while adding more switched capacitor to improve the voltage gain [17-18].

Voltage doubler technique is implemented to attain high voltage ratio. In literature it is used with coupled inductor which helps in recycling the inductive leakage source [19, 20]. The main drawback in inductive frequency is twice the switching frequency. With the

combination of the coupled inductor, voltage lift technique [21, 22] and capacitor diode Voltage Multiplier (VM) technique was implemented in [23-26]. But there was a drawback such as complex structure, high cost and capacitor diode voltage multiplier results in high input ripple current.

Theoretically the conventional boost converter could not produce high voltage step up ratio. So the combination of voltage quadruple and boost converter is designed, so that high voltage ratio is attained with reduced loss and increased efficiency. A predictable converter with single switch provides large ripple current which in turn results in high conduction loss. Henceforth single switch boost converter is combined with voltage quadruple to overcome this consequence [27].

The single switch three diode dc-dc converters with PWM technique is proposed in [28]. The single switch converter design is simple and easy in design with reduced voltage ripple, switch strain and easier control. The quadratic boost converter is also used in high voltage conversion with modest duty cycle. It provides less output efficiency [29]. High step up converters are achieved by the combination of conventional boost converters with sepic and CUK type converters [30].

Sepic converters are also good choice for high voltage step up ratio [31]. The switch voltage stress is less compared to other converter models but the converter efficiency at high load condition is less on comparing with other converter models. It has benefits such as the terminal polarity is positive, feed current is positive, occurs to work in both step-up and step down condition, input current ripple is less [32]. On increasing the voltage gain by varying duty cycle, it results in power dissipation and discontinuous operation [33-34]. The voltage multiplier and voltage quadruple circuit can be used without the inductor which acts as a resonant inductor in the circuit model. Many researchers also show interest in boosting up the renewable energy with different topologies such as CUK-Sepic [35], interleaved boost converter [36-37], MPPT based DC converter [38-41].

This manuscript presents a new high step up single switch converter for improving high voltage gain to balance the utility power using micro-grid technology. The proposed converter is the combination of the VT and the Sepic boost converter. The VT consists of diodes, capacitor, and inductor. The benefits of the converter are high voltage ratio, reduced conduction loss, low voltage strain. The proposed non-isolated for PV application is shown in Fig.2 .The system provides the output of 400 V.

This manuscript is organized as follows: Section 2 discuss about the operation of the converter in continuous and discontinuous mode. Section 3 explains about the analysis part of the converter. Control techniques

of the converter are explained in Section 4 and Section 5 deals with results and discussion. Section 6 is followed by conclusion.

**2. Operating Principle of the Proposed Converter**

The proposed circuit is represented in fig 2. :  
 The converter design consists of main switch  $S_1$ , inductors  $L_1, L_2$ , diodes  $D_1, D_2, D_3$ , and capacitors  $C_1, C_2, C_3$ , and output capacitor  $C_0$ .  
 The VT circuit is combined with sepic converter to increase the voltage gain of the converter. The switching voltage in the semiconductor device is reduced. Capacitors operate as similar operation in conventional boost converter.

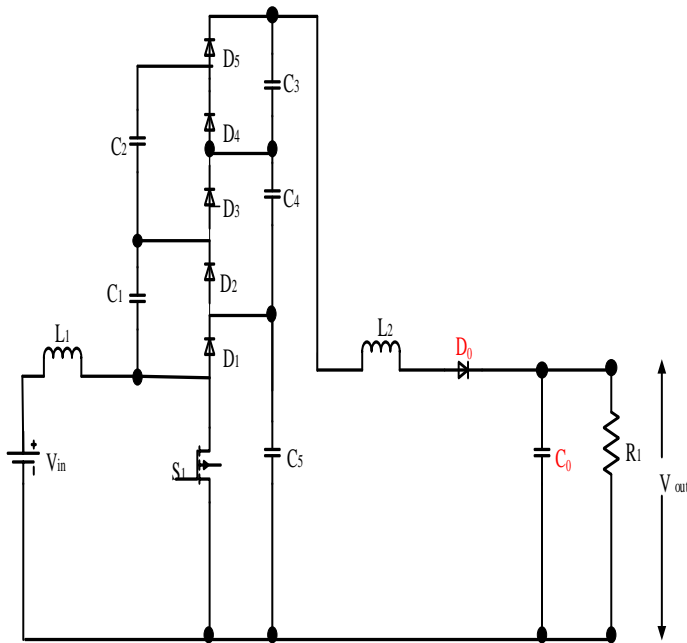


**Fig.2** Proposed single switch DC-DC Converter

**2.1. Continuous conduction mode operation:**

The proposed converter operates in two modes. The modes of operations are shown in Fig.3 and Fig.4

**Mode I [t0-t1]:** When the switch  $S_1$ , is turned ON, diode  $D_1$  and  $D_2$  is turned ON. Diode  $D_3$  and  $D_0$  are reverse biased. The voltage  $V_{in}$  is delivered to  $L_1$  and  $V_{C3} - V_{C2} - V_{C1}$  is delivered to  $L_2$ . These inductors help in storing the energy. The Output capacitor  $C_0$  discharges the required energy to the load for its operation. When the switch turns off, this mode ends. Also the diode  $D_3$  and  $D_0$  current attains zero at  $t=t_1$ .

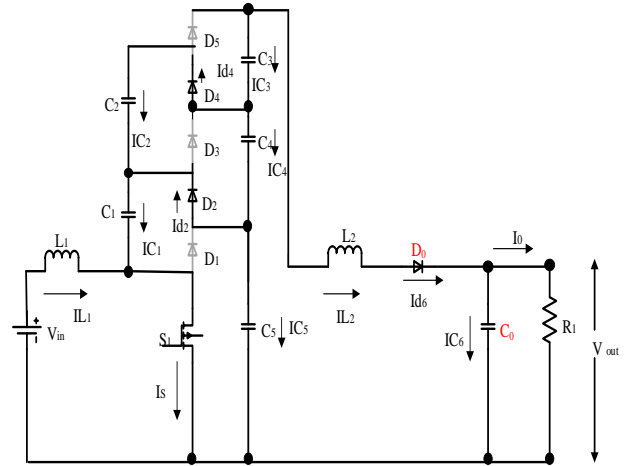


**Fig.3.** Proposed DC-DC converters turn on mode

**Mode II [t1-t2]:** When the switch  $S_2$ , is turned OFF, the diodes  $D_1$  and  $D_2$  are in OFF condition. The diodes  $D_3$  and  $D_0$  are in forward condition. The capacitors are charged by the inductor  $L_1$  and  $L_2$ . The load receives the energy by discharging mode of the capacitor. This operation ends when Switch is turned ON. The next cycle continues.

The main operational waveform is represented in fig. 5. The total capacitive voltage is equal to the output voltage of the converter.

$$V_o = V_{C1} + V_{C2} + V_{C3} + V_{C0} \tag{1}$$

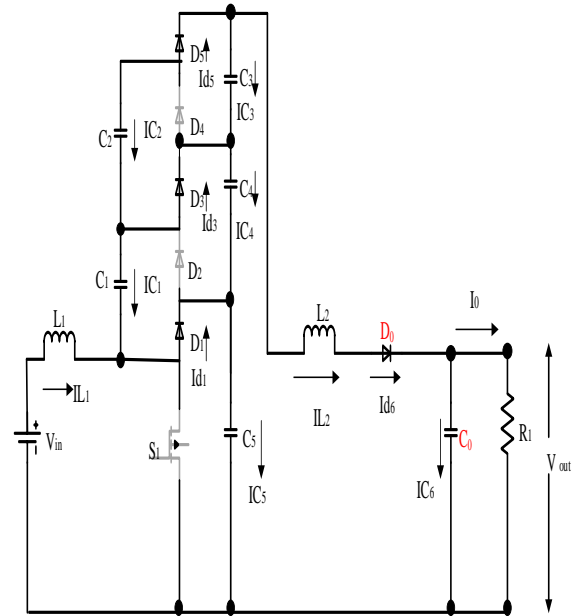


**Fig.4.** Proposed DC-DC converters turn off mode

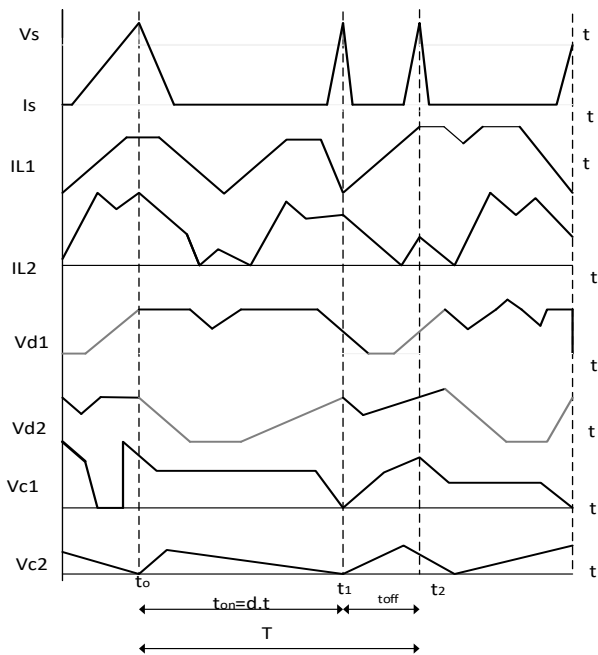


Fig. 5.CCM operation waveforms

2.2. Discontinuous conduction mode of operations:

The DCM mode is performed in three modes for the proposed converter. The operation is explained as follows, *Mode I* [ $t_0-t_1$ ]: When the switch  $S_1$ , is turned ON, diode  $D_1$  and  $D_2$  is turned ON. Diode  $D_3$  and  $D_0$  are reverse biased as represented in fig.3. During the operation  $L_1$  stores energy from input voltage. The inductor  $L_2$  stores the energy of the capacitor. The difference of the capacitive voltage is stored. Hence the voltage across inductors is same as input voltage. The equation is expressed in Eq.2. When switch and diode reaches zero at  $t_1$ , this operation of mode 1 ends.

*Mode II* [ $t_1-t_2$ ]: The Diodes  $D_1, D_2$  are in OFF condition, when the switch  $S_1$  is OFF and other Diodes are in forward biased condition. It is represented in fig.4. This period of converter operation is called conduction time  $T_d$ . The energy stored in mode 1 starts discharging in mode 2. The inductor energy discharges via diodes. The diodes  $D_1$  and  $D_0$ attains zero when the inductive current is same and flows in the same direction.

*Mode III* [ $t_2-t_3$ ]: In this mode of operation, the switch  $S_1$ is turned OFF and all the diodes are in reverse biased operation. The circuit is shown in Fig 6.The waveform is depicted in Fig.7. The inductive voltage becomes Zero; Inductive currents are sustained at constant. So the diodes operate in freewheeling mode. The equation is expressed in Equ 2. The output capacitor  $C_0$  supplies the energy for

the R load to operate. Again the switch moves to turn on and next cycle of mode 1 repeats.

$$\Delta i_{L1} = \Delta i_{L2} = V_{L1} = V_{L2} = 0 \tag{2}$$

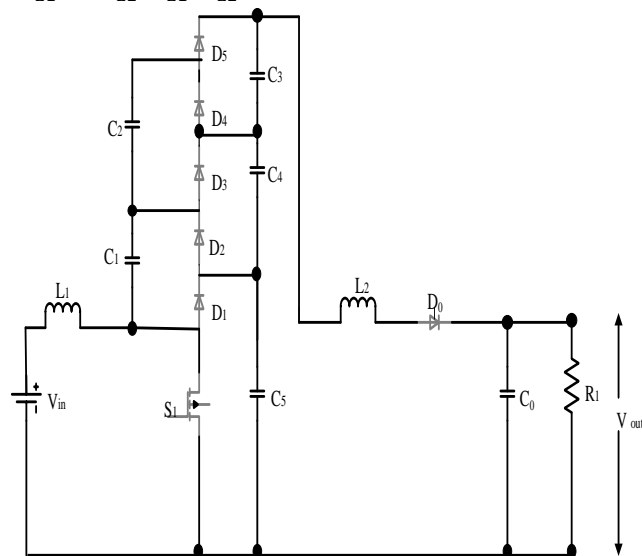


Fig.6. Proposed DC-DC converter DCM mode

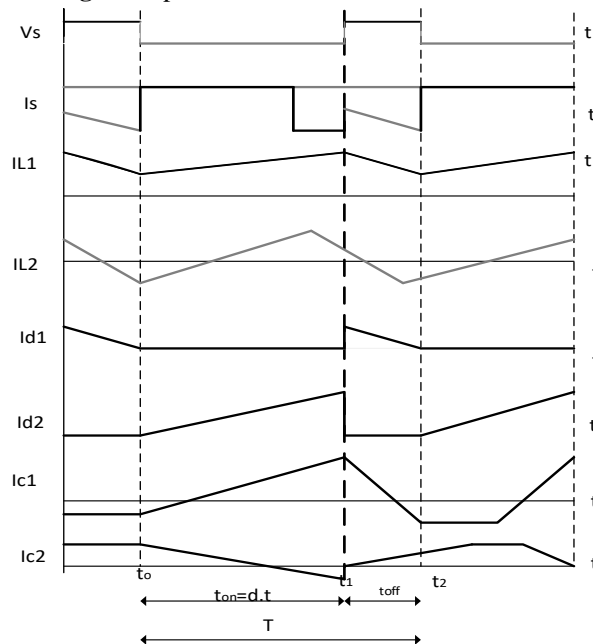


Fig.7 DCM operation waveform

3. Analysis of the Proposed Converter

In this section the theoretical analysis of the proposed sepic converter is explained by following with design procedural of the converter proposed.

3.1 Static gain and switching voltage analysis:

At steady condition, the inductor value is considered as null and the equation is termed as below and hence in CCM operation, the inductor  $L_1$  is given as

$$V_{in} d = V_{c0} - 3V_{in}(1 - d) \tag{3}$$

Here  $d$  is duty cycle, input voltage is  $V_{in}$ . On rearranging the values in Eq. (3), the capacitor  $C_0$  value is obtained same as static gain of the converter.

$$V_{c0} = \frac{3V_{in}}{1-d} \tag{4}$$

The inductor  $L_2$  is zero at steady state condition,

$$(V_{c0} - V_{c1})d = (V_0 - V_{c0})(1 - d) \tag{5}$$

From equation 1, capacitor 1 voltage is given by,

$$V_{c1} = V_0 - V_{c2} - V_{c3} - V_{c0} \tag{6}$$

By substituting the equation 3 & 4 in 5 the static gain is derived as ,

$$\frac{v_0}{v_{in}} = 3(1 + d|1 - d) \tag{7}$$

The duty cycle equation of the converter proposed is given as,

$$\frac{1-d}{d} = 3 \frac{v_{in}}{v_0} \tag{8}$$

The capacitor voltage in  $C_2, C_3$  are given as

$$V_{c2} = \frac{3V_{in}}{1-d} \tag{9}$$

$$V_{c3} = \frac{3V_{in}}{1-d} \tag{10}$$

The static gain is compared with other classical converters in fig. 8. The gain of the proposed converter is high compared to other converters. The gain of the converter is calculated using the output source voltage and input voltage. From fig.9, it is observed that the proposed converter attains required voltage gain with reduced duty cycle  $D=0.814$ . It's given that the switching voltage of the sepic converter is the sum of input and output voltage as of boost converter. The switching voltage of the proposed converter is determined and it is compared with conventional boost converter. As the switching voltage of the proposed converter is less compared with other converters, the switching stress and loss is also less.

3.2 Design analysis of the proposed converter:

On the basis of the analytical expression of the converter operation, the component design values are selected [11].

1) Duty cycle calculation:

The proposed converters step up and step down of voltage varies due to the duty cycle control. And also it is dependent on elements in the circuit. The output of the proposed converter is given as,

$$v_0 = \frac{D*3v_{in}}{1-D} \tag{11}$$

On taking the diode voltage drop in to account,

$$v_0 + v_D = \frac{D*3v_{in}}{1-D} \tag{12}$$

On simplifying,

$$D = \frac{v_0 + v_D}{v_0 + 3v_{in} + v_D} \tag{13}$$

The attained duty cycle is 0.81.

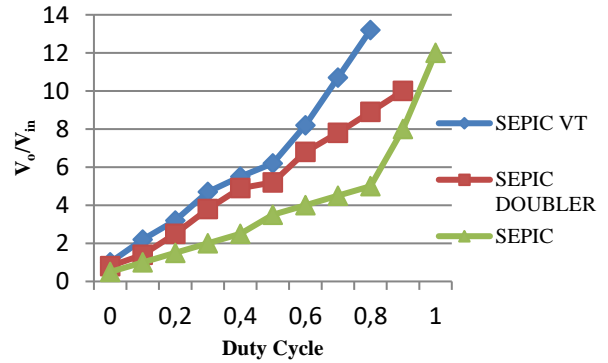


Fig.8 Static gain analysis

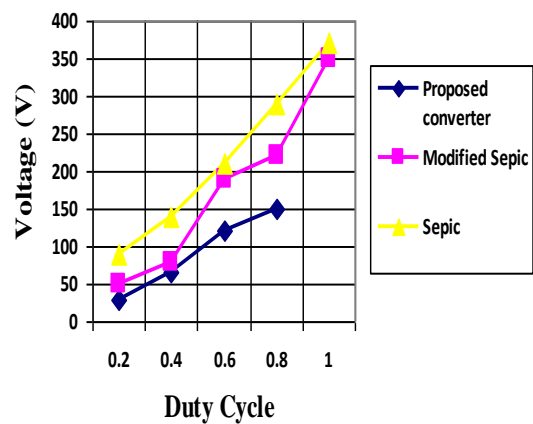


Fig.9 Switching voltage of proposed converter

2) Inductor Selection:

The inductance values are identified with the help of input current ripples [11]. i.e.  $\Delta I_{L1}$  and  $\Delta I_{L2}$ . The values of the input current ripples are 1.77 A .

$$L_1 = \frac{D*3v_{in}}{f.\Delta I_{L1}} \tag{14}$$

$$L_2 = \frac{1-D*v_{c2}}{f.\Delta I_{L2}} \tag{15}$$

$$I_{ripple} = I_{out} \times \frac{V_{out}}{3v_{in}} \times 40\% \tag{16}$$

3) Capacitor Selection:

Voltage ripple ( $\Delta v_c$ ) is used to calculate the capacitance value. The ripple value is obtained by the 10% of the input voltage value. The capacitive ripple current is obtained using

eq.19 and the ripple current is 2.108 A. The formula to obtain the capacitor value is given by,

$$c_1 = c_2 = c_3 = \frac{I_0}{f \cdot \Delta v_c} \quad (17)$$

The ripple voltage is obtained by,

$$\Delta v_c = \frac{v_{in}}{1-d} * 10\% \quad (18)$$

The ripple capacitive current is attained by,

$$I_{cs} = I_0 \times \sqrt{\frac{V_0}{3V_{in}}} \quad (19)$$

4) *Output capacitor:*

The output capacitor  $c_0$  is designed as same as boost converter design. To calculate the output capacitor frequency  $f_c$ , output power  $p_0$ , output voltage  $v_0$  and output ripple voltage  $\Delta v_0$ . 1% of output voltage is equal to output ripple voltage. The capacitance is calculated using

$$c_0 = \frac{p_0}{4\pi f_g v_0 \Delta v_0} \quad (20)$$

5) *Component stress:*

The component design purpose the switch current  $i_1$  and  $i_2$  at the turn ON and end of turn ON is found using below equation [11]. On taking the theoretical efficiency value = 98% . Here the RMS current of the switch( $i_{rms}$ )

$$i_1 = \left( \frac{p_0}{\eta * v_{in}} - \frac{\Delta I_L}{2} \right) + \left( i_0 - \frac{\Delta I_L}{2} \right) \quad (21)$$

$$i_2 = \left( \frac{p_0}{\eta * v_{in}} + \frac{\Delta I_L}{2} \right) + \left( i_0 + \frac{\Delta I_L}{2} \right) \quad (22)$$

$$i_{rms} = \sqrt{\frac{1}{3} \cdot (i_1^2 + i_2^2 + i_1 \cdot i_2) \cdot d} \quad (23)$$

The output current ( $i_0$ ) is same as diode current  $i_{D1}$ ,  $i_{D2}$  and  $i_{D0}$

$$i_0 = i_{D1} = i_{D2} = i_{D0} = \frac{p_0}{v_0} \quad (24)$$

3.3) *Comparison of proposed converter with conventional converter:*

**Table 1:** Comparison of converter formulas [27].

Param eters	Boost converter	Sepic	Modified Sepic	Proposed converte r
Switch duty cycle [27]	$D = 1 - \frac{V_{in}}{V_{out}}$	$D = \frac{V_{out}}{V_{out} + V_{i}}$	$D = \frac{V_{out} - V_{in}}{V_{out} + V_{in}}$	$D = \frac{v_0 + v_D}{v_0 + 3v_{in} + v_D}$
Induct ance [27]	$L = \frac{V_{out} \cdot D}{\Delta I_L \cdot f}$	$L_1 = L_2 = \frac{V_{out} \cdot D}{\Delta I_L \cdot f}$	$L_1 = L_2 = \frac{V_{out} \cdot D}{\Delta I_L \cdot f}$	$L_1 = \frac{D * 3v_{in}}{f \cdot \Delta I_{L1}}$ $L_2 = \frac{1 - D *}{f \cdot \Delta I_L}$
Capaci tors [27]	$C_0 = \frac{D}{R \left( \frac{\Delta V_0}{V} \right)}$	$C_1 = C_0 = \frac{D}{R \left( \frac{\Delta V_0}{V} \right)}$	$C_s = \frac{I_{out}}{\Delta V_c \cdot f}$ $C_1 = C_2 = \frac{D}{R \left( \frac{\Delta V_0}{V} \right)}$	$c_0 = \frac{p_0}{4\pi f_g v_0^4}$ $c_1 =$ $c_2 =$ $c_3 = \frac{I_0}{f \cdot \Delta v_c}$

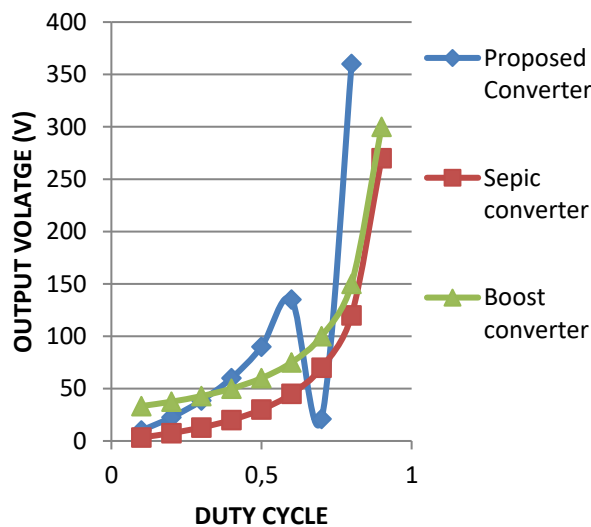


**Fig.10** Converter output voltage

On comparing the proposed converter with conventional converter, the step up of voltage range is high. The comparison chart depending on output voltage is depicted in Fig.10 and the formula comparison is depicted in table.1.

**4. Small Signal Analysis**

The proposed converter is designed for an average circuit model and it is represented in fig 11. depending on switching period. Switching average current is depicted by eq. 25 and diode voltage is depicted by eq. 26.

$$(i_s)T_s = s = di_{L1} + \frac{V_0}{R} \tag{25}$$

$$(v_{d1})T_s, (v_{d2})T_s, (v_{d3})T_s = E_{d1} = E_{d1} = E_{d1} = (1 - d)(V_0 - V_{c1}) \tag{26}$$

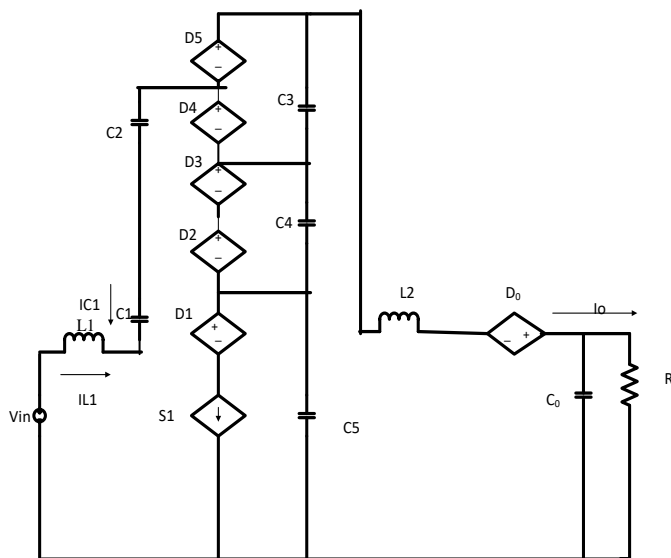


**Fig.11** Average circuit design of proposed converter

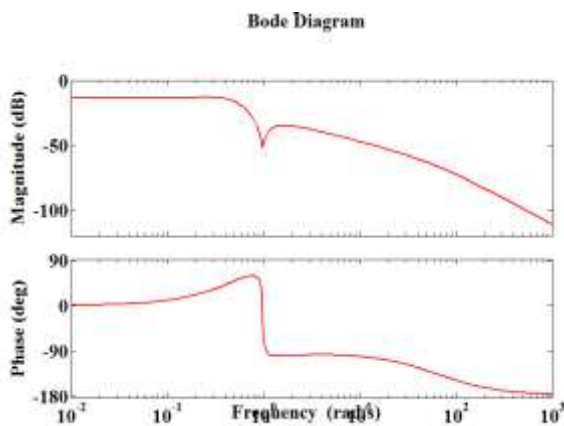


**Fig.12** Frequency response of proposed converter

This circuit is utilized to derive the transfer function of the converter and to process the analysis of frequency response of the converter. The frequency response analysis is depicted in fig.12. The analysis is plotted between input and output voltage sources. The bode -plot exhibits the stability of the proposed converter. The proposed converter is stable over the variation in the input voltage. The gain of

the converter remains constant as though the input power changes.

The transfer function obtained using the average signal model is ,

$$tf = \frac{2.75e^{-5}s^3 + 1.101e^7s^2 + 2.583e^{17}s^1 + 1.192e^6}{s^5 + 62.53s^4 + 8.596s^3 + 5.292e^{11}s^2 + 1.017e^{19}s^1 + 5.87e^{20}} \tag{27}$$

The maximum peak over shoot is 0% in this converter. The settling time attained is 0.2 sec. The steady state of the converter is attained below 0.5 secs.

**5. Results and Discussion:**

In this section the results of proposed converter is compared with conventional. The settling time, peak time and steady state error is analysed. The output voltage and current waveform of the proposed converter is represented in Fig 13. The two control techniques PI and fuzzy are utilized to check the working condition of the proposed converter. The PI is a classical model controller where the control action is done by tuning the parameters. Fuzzy is a rule base controller which controls the duty cycle to control the output voltage of the converter. Analyses are made by simulations. This study is carried out utilizing Simulink with parameters represented in table 2.

**Table 2:** Parameters of the proposed converter

Components	Parameter
Input voltage	30 V
Output voltage	400 V
Input current	15.2 A
Output current	1 A
Inductor L <sub>1</sub> , L <sub>2</sub>	205, 180 μH
Capacitor C <sub>1</sub> , C <sub>2</sub> , C <sub>4</sub>	2.2 μF
Capacitor C <sub>3</sub>	2.2 μF
Capacitor C <sub>0</sub>	40 μF
Resistor	400 Ω

The output voltage waveform and current waveform is depicted in fig.13 and fig.14. Here the 30V is boosted to 400V with stable waveform. The transient response of this proposed converter is good on comparing with the boost and other conventional converters. The efficiency attained by the proposed converter is also high compared to other conventional converter.

The diode voltage, switching voltage, capacitive voltage are depicted in fig 15, 16,17. In fig.18 the efficiency of the proposed converter is compared with other conventional converters. On comparing with the boost and sepic converter the proposed converter

efficiency is high. The overall analysis shows that the proposed converter is good for PV energy conversion since it has less conduction and switching loss, reduced number of switch and size of the converter. The ripple voltage attained is less on comparing with other converters. The efficiency of the converter is also high since the losses are minimized. This converter will be suitable for inverter process to convert the dc source to ac source. The design process of the proposed converter is detailed in Table 3:

The main benefits of the converter are the size of the converter is reduced with single switch. The steady state response of the converter is attained. The high voltage conversion is attained at moderate duty cycle with reduced ripple current. These are all depicted in the simulation analysis from fig 13-17.

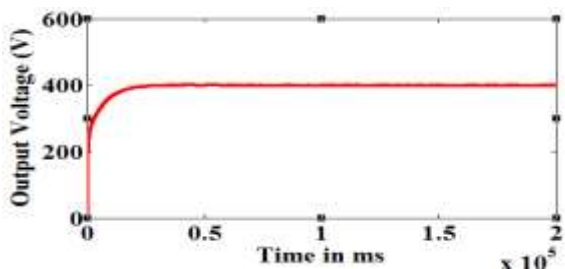


Fig.13 Output voltage

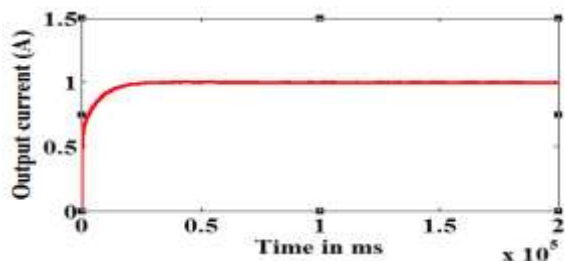


Fig.14 Output current

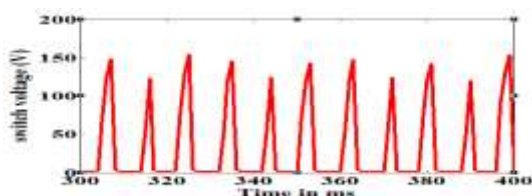


Fig.15 a) Switch voltage

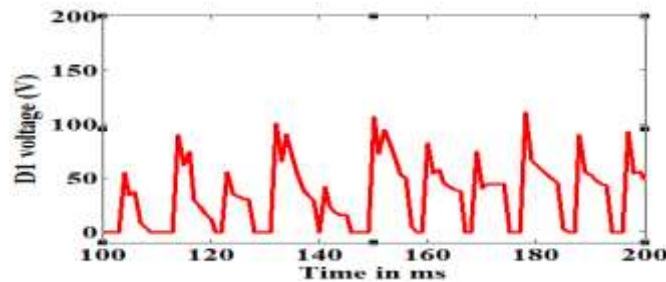


Fig.15 b) Diode 1 voltage

Components	Formula used	Parameter range for simulation	Hardware parameter
Inductor L1,L2	$L_1 = \frac{D * 3v_{in}}{f * \Delta I_{L1}}$ $L_2 = \frac{1 - D * v_{c2}}{f * \Delta I_{L2}}$	$L_1 = 180 \mu\text{H}$ $L_2 = 150 \mu\text{H}$	$L_1 = 205 \mu\text{H}$ $L_2 = 180 \mu\text{H}$
capacitor	$c_0 = \frac{p_0}{4\pi f_g v_0 \Delta v_0}$ $c_1 = c_2 = c_3 = \frac{I_0}{f \Delta v_c}$	$c_1 = c_2 = c_3 = 2.2 \mu\text{F}$ $c_0 = 40 \mu\text{F}$	$c_1 = c_2 = c_3 = 2.2 \mu\text{F}$ $c_0 = 40 \mu\text{F}$
Switch duty cycle	$D = \frac{v_o + v_D}{v_o + 3v_{in} + v_D}$	$D = 0.81$	$D = 08.1$

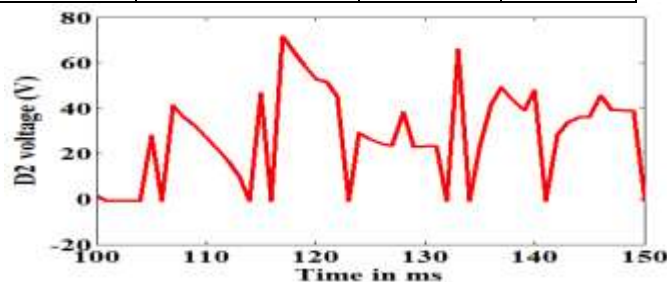


Fig.15 c) Diode 2 voltage

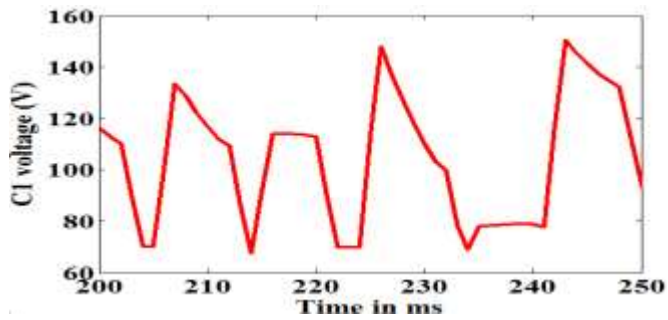


Fig.16 a) C1 capacitive voltage

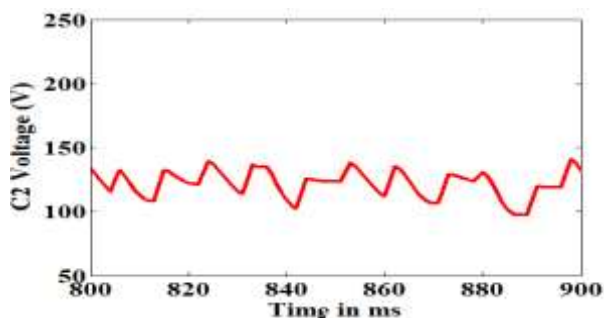


Fig.16 b) C2 capacitive voltage

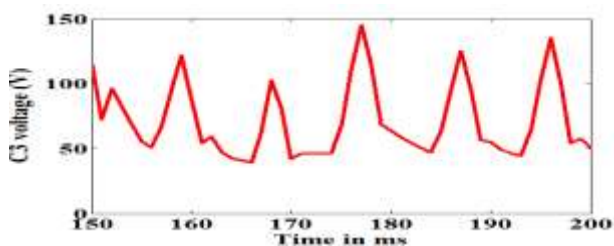


Fig.16 c) C3 capacitive voltage

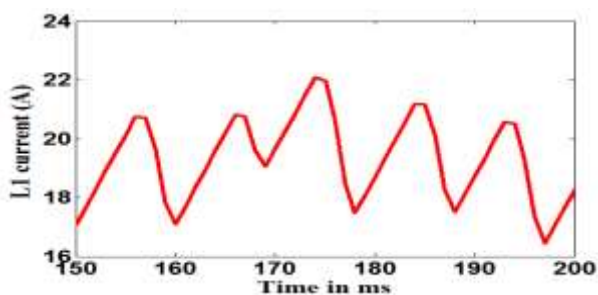


Fig.17 a) L1 inductive current

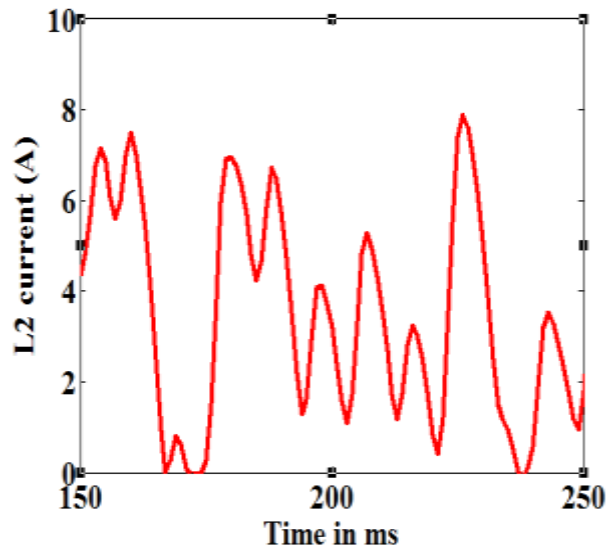


Fig.17 b) L2 inductive current

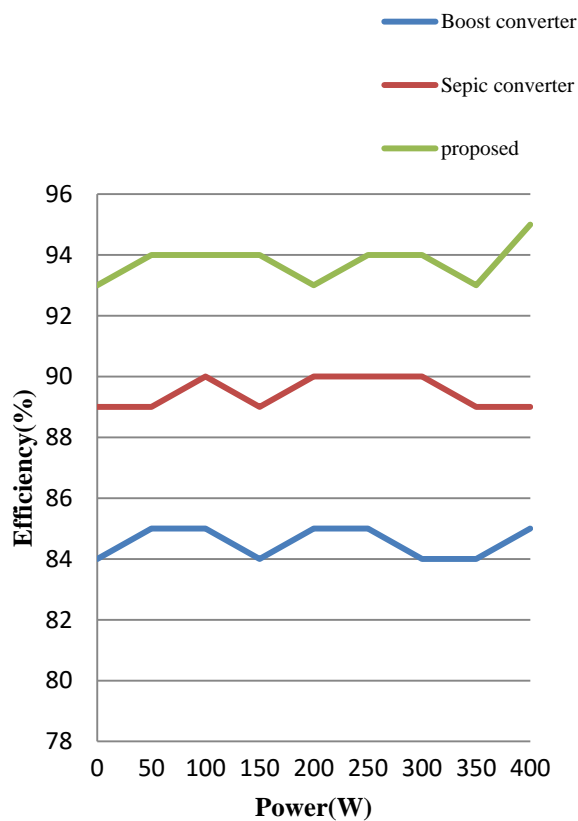
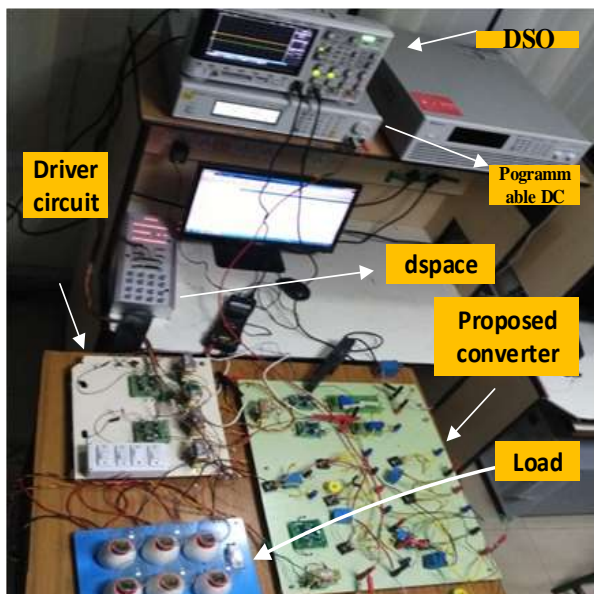


Fig.18 Comparison of efficiency with other converters

## 6. Hardware Results

The designed converter is tested experimentally in laboratory and the fig. 19 illustrates the experimental analysis. The simulation results and the hardware results are similar. The results obtained in simulation are same as

results obtained in hardware. The ripple voltage and the voltage gain attained is same. Also the transient response analysis attained in simulation is same as the results attained in hardware. The output voltage and the output currents are depicted in the fig .20. The maximum peak over shoot is absent in the hardware analysis too. The output ripple voltage is minimized and it is experimentally proved. The steady atate is represented in fig.21.



**Fig. 19** Hardware prototype

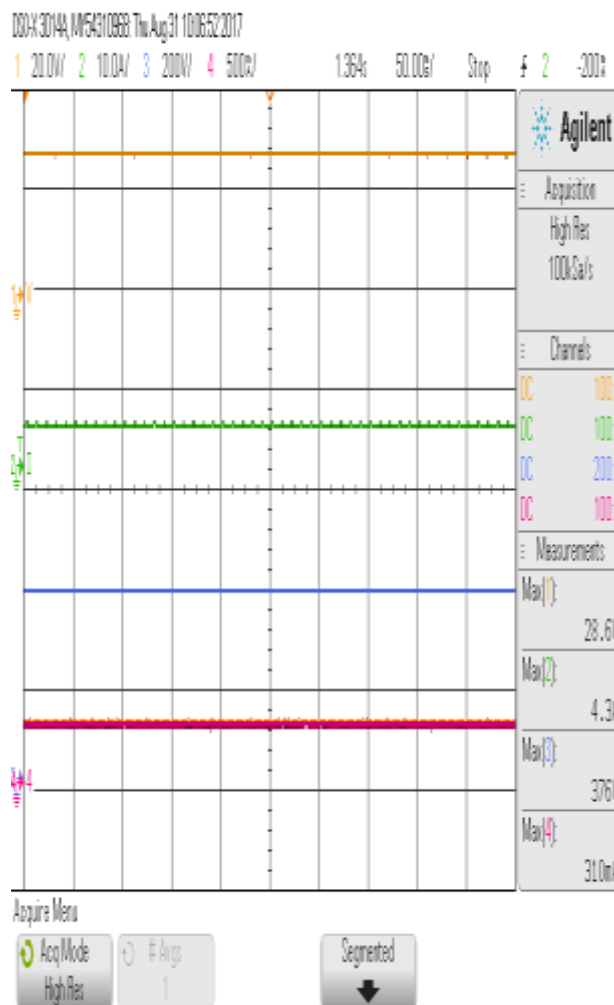


**Fig.21** Steady state representation of the proposed converter

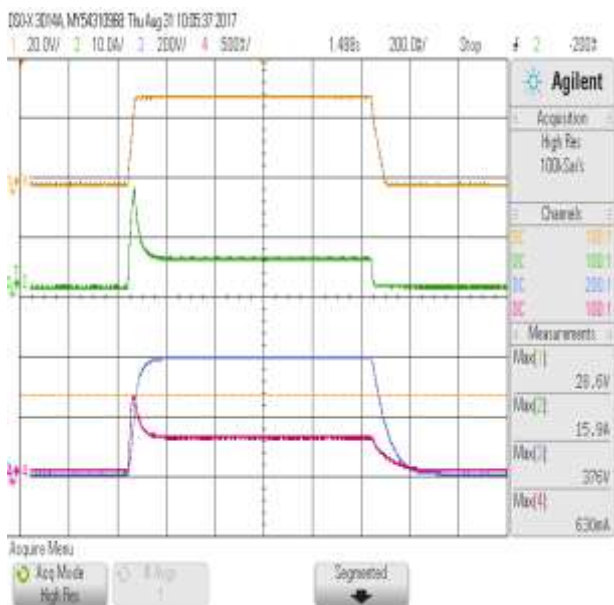


**Fig.20** Output voltage and current representation

## 7. Conclusion

In this manuscript, a single switch VT DC-DC converter is proposed. The CCM and DCM mode operation is explained in detail with the waveform. The mathematical expression for the proposed converter is derived and analyzed with the simulation results. Also the proposed converter is compared with other conventional converter in the basis of efficiency and the output power. In this designed converter the duty cycle attained is 0.81 and the ripple current is reduced to 1.3 Amps. The main advantage such as reduced size of the converter, reduced number of switch, reduced ripple current is attained. This converter has high efficiency while switching and conduction loss is less. The single switch converter has a special feature compared to other model converter. The efficiency attained is stable on comparing to other converters. This converter is suitable for PV energy conversion and it is also suitable to connect to the inverter source. This can be analysed through hardware results in future.

## References

- [1] Chen, Shih-Ming, Tsorng-Juu Liang, Lung-Sheng Yang, and Jiann-Fuh Chen. "A cascaded high step-up DC–DC converter with single switch for microsource applications." *IEEE Transactions on Power Electronics* 26, no. 4 (2011): 1146-1153.
- [2] Fleming, Eric M., and Ian A. Hiskens. "Dynamics of a microgrid supplied by solid oxide fuel cells." In *Bulk Power System Dynamics and Control-VII. Revitalizing Operational Reliability, 2007 iREP Symposium*, pp. 1-10. IEEE, 2007.
- [3] Ito, Youichi, Yang Zhongqing, and Hirofumi Akagi. "DC microgrid based distribution power generation system." In *Power Electronics and Motion Control Conference, 2004. IPENC 2004. The 4th International*, vol. 3, pp. 1740-1745. IEEE, 2004.
- [4] Wang, Baochao, Manuela Sechilariu, and Fabrice Locment. "Intelligent DC microgrid with smart grid communications: Control strategy consideration and design." *IEEE transactions on smart grid* 3, no. 4 (2012): 2148-2156.
- [5] Veneri, Ottorino, Clemente Capasso, and Diego Iannuzzi. "Experimental evaluation of DC charging architecture for fully-electrified low-power two-wheeler." *Applied Energy* 162 (2016): 1428-1438.
- [6] Sun, Yao, Chaolu Zhong, Xiaochao Hou, Jian Yang, Hua Han, and Josep M. Guerrero. "Distributed cooperative synchronization strategy for multi-bus microgrids." *International Journal of Electrical Power & Energy Systems* 86 (2017): 18-28.
- [7] Tiwari, Ramji, and N. Ramesh Babu. "Recent developments of control strategies for wind energy conversion system." *Renewable and Sustainable Energy Reviews* 66 (2016): 268-285.
- [8] Li, Wuhua, and Xiangning He. "Review of nonisolated high-step-up DC/DC converters in photovoltaic grid-connected applications." *IEEE Transactions on Industrial Electronics* 58, no. 4 (2011): 1239-1250.
- [9] Kim, Jae-Kuk, and Gun-Woo Moon. "Derivation, analysis, and comparison of nonisolated single-switch high step-up converters with low voltage stress." *IEEE Transactions on Power Electronics* 30, no. 3 (2015): 1336-1344.
- [10] Choi, Woo-Young, and Change-Goo Lee. "Photovoltaic panel integrated power conditioning system using a high efficiency step-up DC–DC converter." *Renewable energy* 41 (2012): 227-234.
- [11] Saravanan, S., and N. Ramesh Babu. "Analysis and implementation of high step-up DC-DC converter for PV based grid application." *Applied Energy* 190 (2017): 64-72.
- [12] Freitas, Antônio Alisson Alencar, Fernando Lessa Tofoli, Edilson Mineiro Sá Júnior, Sergio Daher, and Fernando Luiz Marcelo Antunes. "High-voltage gain dc–dc boost converter with coupled inductors for photovoltaic systems." *IET Power Electronics* 8, no. 10 (2015): 1885-1892.
- [13] Khalilzadeh, Mohammad, and Karim Abbaszadeh. "Non-isolated high step-up DC–DC converter based on coupled inductor with reduced voltage stress." *IET Power Electronics* 8, no. 11 (2015): 2184-2194.
- [14] Nouri, Tohid, Seyed Hossein Hosseini, Ebrahim Babaei, and Jaber Ebrahimi. "A non-isolated three-phase high step-up DC–DC converter suitable for renewable energy systems." *Electric Power Systems Research* 140 (2016): 209-224.
- [15] Wu, Gang, Xinbo Ruan, and Zhihong Ye. "Nonisolated high step-up DC–DC converters adopting switched-capacitor cell." *IEEE Transactions on Industrial Electronics* 62, no. 1 (2015): 383-393.
- [16] Poorali, Behzad, Arash Torkan, and Ehsan Adib. "High step-up Z-source DC–DC converter with coupled inductors and switched capacitor cell." *IET Power Electronics* 8, no. 8 (2015): 1394-1402.
- [17] Ajami, Ali, Hossein Ardi, and Amir Farakhor. "A novel high step-up DC/DC converter based on integrating coupled inductor and switched-capacitor techniques for renewable energy applications." *IEEE Transactions on Power Electronics* 30, no. 8 (2015): 4255-4263.
- [18] Tang, Yu, Dongjin Fu, Ting Wang, and Zhiwei Xu. "Hybrid switched-inductor converters for high step-up conversion." *IEEE Transactions on Industrial Electronics* 62, no. 3 (2015): 1480-1490.
- [19] Zhao, Yi, Wuhua Li, and Xiangning He. "Single-phase improved active clamp coupled-inductor-based converter with extended voltage doubler cell." *IEEE Transactions on Power Electronics* 27, no. 6 (2012): 2869-2878.
- [20] Yang, Lung-Sheng, Tsorng-Juu Liang, Hau-Cheng Lee, and Jiann-Fuh Chen. "Novel high step-up DC–DC converter with coupled-inductor and

- voltage-doubler circuits." *IEEE Transactions on industrial Electronics* 58, no. 9 (2011): 4196-4206.
- [21] Zhu, M. U., and F. L. Luo. "Series SEPIC implementing voltage-lift technique for DC-DC power conversion." *IET Power Electronics* 1, no. 1 (2008): 109-121.
- [22] Changchien, S-K., T-J. Liang, J-F. Chen, and L-S. Yang. "Step-up DC-DC converter by coupled inductor and voltage-lift technique." *IET power electronics* 3, no. 3 (2010): 369-378.
- [23] Sizkoohi, Hadi Moradi, Jafar Milimonfared, Meghdad Taheri, and Sina Salehi. "High step-up soft-switched dual-boost coupled-inductor-based converter integrating multipurpose coupled inductors with capacitor-diode stages." *IET Power Electronics* 8, no. 9 (2015): 1786-1797.
- [24] Hu, Xuefeng, and Chunying Gong. "A high voltage gain DC-DC converter integrating coupled-inductor and diode-capacitor techniques." *IEEE transactions on power electronics* 29, no. 2 (2014): 789-800.
- [25] Young, Chung-Ming, Sheng-Feng Wu, Ming-Hui Chen, and Sing-Jhao Chen. "Single-phase ac to high-voltage dc converter with soft-switching and diode-capacitor voltage multiplier." *IET Power Electronics* 7, no. 7 (2014): 1704-1713.
- [26] Liang, Tsorng-Juu, Shih-Ming Chen, Lung-Sheng Yang, Jiann-Fuh Chen, and Adrian Ioinovici. "Ultra-large gain step-up switched-capacitor DC-DC converter with coupled inductor for alternative sources of energy." *IEEE Transactions on Circuits and Systems I: Regular Papers* 59, no. 4 (2012): 864-874.
- [27] Saravanan, S., and N. Ramesh Babu. "RBFN based MPPT algorithm for PV system with high step up converter." *Energy Conversion and Management* 122 (2016): 239-251.
- [28] Gules, Roger, Walter Meneghette dos Santos, Flavio Aparecido dos Reis, Eduardo Felix Ribeiro Romaneli, and Alceu Andre Badin. "A modified SEPIC converter with high static gain for renewable applications." *IEEE transactions on power electronics* 29, no. 11 (2014): 5860-5871.
- [29] de Melo, Priscila Facco, Roger Gules, Eduardo Félix Ribeiro Romaneli, and Rafael Christiano Annunziato. "A modified SEPIC converter for high-power-factor rectifier and universal input voltage applications." *IEEE Transactions on Power Electronics* 25, no. 2 (2010): 310-321.
- [30] Pires, V. Fernão, Daniel Foito, F. R. B. Baptista, and J. Fernando Silva. "A photovoltaic generator system with a DC/DC converter based on an integrated Boost-Cuk topology." *Solar Energy* 136 (2016): 1-9.
- [31] Wai, Rong-Jong, and Rou-Yong Duan. "High step-up converter with coupled-inductor." *IEEE Transactions on Power Electronics* 20, no. 5 (2005): 1025-1035.
- [32] Wai, Rong-Jong, Chung-You Lin, Rou-Yong Duan, and Yung-Ruei Chang. "High-efficiency DC-DC converter with high voltage gain and reduced switch stress." *IEEE Transactions on Industrial Electronics* 54, no. 1 (2007): 354-364.
- [33] Changchien, Shih-Kuen, Tsorng-Juu Liang, Jiann-Fuh Chen, and Lung-Sheng Yang. "Novel high step-up DC-DC converter for fuel cell energy conversion system." *IEEE Transactions on Industrial Electronics* 57, no. 6 (2010): 2007-2017.
- [34] Arunkumari, T., and V. Indragandhi. "An overview of high voltage conversion ratio DC-DC converter configurations used in DC micro-grid architectures." *Renewable and Sustainable Energy Reviews* 77 (2017): 670-687.
- [35] Kumar, K., Babu, N.R. and Prabhu, K.R., 2017. Design and Analysis of an Integrated Cuk-SEPIC Converter with MPPT for Standalone Wind/PV Hybrid System. *International Journal of Renewable Energy Research (IJRER)*, 7(1), pp.96-106.
- [36] Addula, S.R. and Mahalingam, P., 2016. Coupled Inductor Based Soft Switched Interleaved DC-DC Converter for PV Applications. *International Journal of Renewable Energy Research (IJRER)*, 6(2), pp.361-374.
- [37] RAMASAMY, S., Abishri, P. and Umashankar, S., 2016. Review of Coupled Two and Three Phase Interleaved Boost Converter (IBC) and Investigation of Four Phase IBC for Renewable Application. *International Journal of Renewable Energy Research (IJRER)*, 6(2), pp.421-434.
- [38] Jayalakshmi, N.S., Gaonkar, D.N. and Naik, A., 2017. Design and Analysis of Dual Output Flyback Converter for Standalone PV/Battery System. *International Journal of Renewable Energy Research (IJRER)*, 7(3), pp.1032-1040.
- [39] Poshtkouhi, S. and Trescases, O., 2011, March. Multi-input single-inductor dc-dc converter for MPPT in parallel-connected photovoltaic applications. In *Applied Power Electronics Conference and Exposition (APEC), 2011 Twenty-Sixth Annual IEEE* (pp. 41-47). IEEE.
- [40] Ikeda, S. and Kurokawa, F., 2017, October. Isolated and wide input ranged boost full bridge DC-DC converter with low loss active snubber.

In Energy Conversion Congress and Exposition (ECCE), 2017 IEEE (pp. 2213-2218). IEEE.

- [41] Li, F., Alshareef, M., Lin, Z. and Jiang, W., 2016, November. A modified MPPT algorithm with integrated active power control for PV-battery systems. In Renewable Energy Research and Applications (ICRERA), 2016 IEEE International Conference on (pp. 742-746). IEEE.